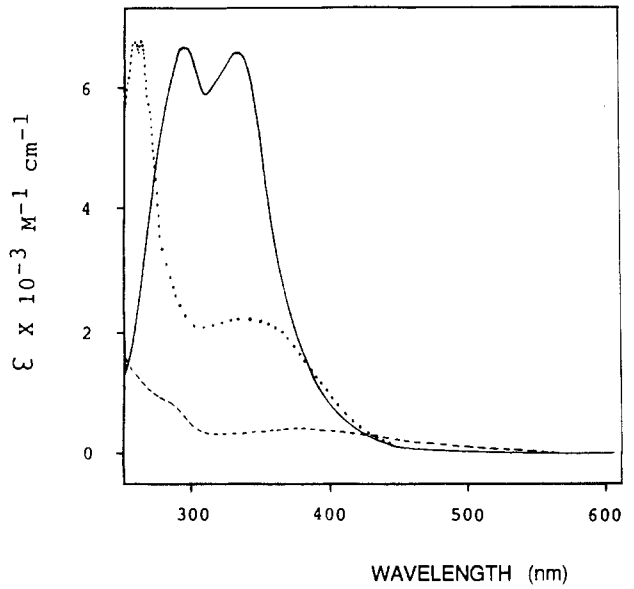

Figure 4. Uv-visible spectra at pH = 1 of $[(tpm)Ru^{II}(H_2O)_3]^{2+}$ (—), of electrochemically generated $[(tpm)Ru^{III}(H_2O)_3]^{3+}$ (n = 0.9) (···), and of $[(tpm)Ru^{IV}(O)(H_2O)_2]^{2+}$ (---) generated by adding 2 equiv of Ce(IV) to $[(tpm)Ru^{II}(H_2O)_3]^{2+}$.

of the Ru(IV) complex, generated chemically by adding 2 equiv of Ce(IV) to $[(tpm)Ru^{II}(H_2O)_3]^{2+}$, an absorption band of low intensity appears at 374 nm (ϵ = 408). The $\pi \rightarrow \pi^*$(tpm) transition is further shifted to higher energy and is not shown in the spectrum.

The ^{1}H NMR spectrum of the triaquaruthenium complex **1** in D_2O was assigned[19] (the assignments are listed in the Experimental Section) by taking advantage of the symmetry of the molecule. The three pyrazolyl rings of the tpm ligand are equivalent, which greatly simplifies integrations. The methylenic proton of the tpm ligand is not observed in the spectrum due to a fast-exchange process with D_2O. In 0.1 M DCl a new resonance appears at 9.2 ppm (s, 1), which can be assigned to this proton. This resonance does not appear in 0.1 M NaOD. From the absence of shifts in the remaining resonances, it can be inferred that anation by Cl^- is relatively unimportant under these conditions.

Acknowledgments are made to the National Science Foundation under Grant No. CHE-8601604 and the National Institutes of Health under Grant No. GM32296 for support of this research. A.L. acknowledges support from a Fulbright "La Caixa" Fellowship (Barcelona, Spain).

Registry No. **1**, 128824-20-4; **2**, 128824-24-8; $[(tpm)Ru(H_2O)_3]^{3+}$, 128824-21-5; $[(tpm)Ru(H_2O)_3]^{4+}$, 128824-22-6; $[(tpm)Ru(H_2O)_3]^{5+}$, 128824-23-7.

Supplementary Material Available: Listings of hydrogen atom positions and anisotropic thermal parameters (4 pages); a table of observed and calculated structure amplitudes (24 pages). Ordering information is given on any current masthead page.

(19) Pretsch, E.; et al. *Tables of Spectral Data for Structure Determination of Organic Compounds*; Springer-Verlag: West Berlin, 1983.

Contribution from the Chemistry Department,
The Ohio State University, Columbus, Ohio 43210

Inclusion Complex Formation Involving a New Class of Transition-Metal Host

Thomas J. Meade, Nathaniel W. Alcock, and Daryle H. Busch*

Received November 7, 1989

This new class of transition-metal-containing host molecule readily accommodates aromatic rings as guests. The complexation is regiospecific and driven by hydrophobic interactions in aqueous media. Crystallographic data have confirmed the expanded cavity size and the nature of the new hosts. An experimentally justified NMR relaxation technique provided structural information about the guest-host complex in solution. Crystal data for the supervaulted host $[Ni\{Me_2(bipiperidiniumyl)_2$-9,10-anthra[16]-cyclidene$\}](PF_6)_2$: space group $P2_1/c$, a = 14.172 (4) Å, b = 16.235 (5) Å, c = 34.705 (10) Å, β = 109.76°, Z = 4, R = 0.112 for 1775 observed reflections.

Introduction

The field of host-guest chemistry continues to enjoy increasing importance as a vehicle for the study of catalysis, enzyme modeling, and facilitated transport. Several intensively studied classes of hosts, including cyclodextrins, cavitands, and cryptates,[1] form inclusion complexes characterized by the absence of covalent bond formation.[2] Enzymes such as cytochrome P-450[2] exploit hydrophobic interactions as the driving force for enzyme-substrate binding,[3,4] and it is on these interactions that this work and previous work in our laboratory have focused.

The development by Takeuchi of the macrobicyclic ligands known as vaulted cyclidenes led to a credible model of the ternary complex of cytochrome P-450[5-7] (Figure 1). The metal cyclidene hosts bind small organic molecules regiospecifically,[8,9] while simultaneously providing a vacant coordination site on the metal atom for the coordination of dioxygen. Previous NMR chemical shift studies on aqueous solutions first demonstrated host-guest association[5-7] by these transition metal complexes. The copper(II)

* To whom correspondence should be addressed at the Department of Chemistry, University of Kansas, Lawrence, KS 66045-0046.

(1) For reviews, see: (a) Szejtli, J. *Cyclodextrins and Their Inclusion Complexes*; Akademiai Kiado: Budapest, 1982; 296 pp. (b) Tabushi, I. *Tetrahedron* **1984**, *40*, 269. (c) Rossa, L.; Vogtle, F. *Topics in Current Chem.* **1983**, *113*, 1. (d) Cram, D. J. *Science* **1983**, *219*, 1177. Meade, T. J.; Busch, D. H. *Prog. Inorg. Chem.* **1985**, *33*, 59.
(2) Sato, R.; Omura, T. *Cytochrome P-450*; Academic Press: New York, 1978.
(3) (a) White, R. E.; Coon, M. J. *Annu. Rev. Biochem.* **1980**, *49*, 314. (b) White, R. E.; Oprian, D. D.; Coon, M. J. In *Microcomes, Drug Oxidations, and Chemical Carcinogenesis*; Coon, M. J., Connery, A. H., Estabrook, R. W., Gelboin, H., Gillette, J. R., O'Brien, P. J., Eds.; Academic Press: New York, 1980; p 243.
(4) Poulos, T. L.; Finzel, B. C.; Gunsalus, I. C.; Wagner, G. C.; Kraut, J. *J. Biol. Chem.* **1985**, *25*, 16122.
(5) Takeuchi, K. J.; Busch, D. H.; Alcock, N. J. *J. Am. Chem. Soc.* **1981**, *103*, 2421.
(6) Takeuchi, K. J.; Busch, D. H.; Alcock, N. J. *J. Am. Chem. Soc.* **1983**, *105*, 4261.
(7) Takeuchi, K. J.; Busch, D. H. *J. Am. Chem. Soc.* **1983**, *105*, 6812.
(8) Kwik, W.-L.; Herron, N.; Takeuchi, K.; Busch, D. H. *J. Chem. Soc., Chem. Commun.* **1983**, 409.

0020-1669/90/1329-3766$02.50/0

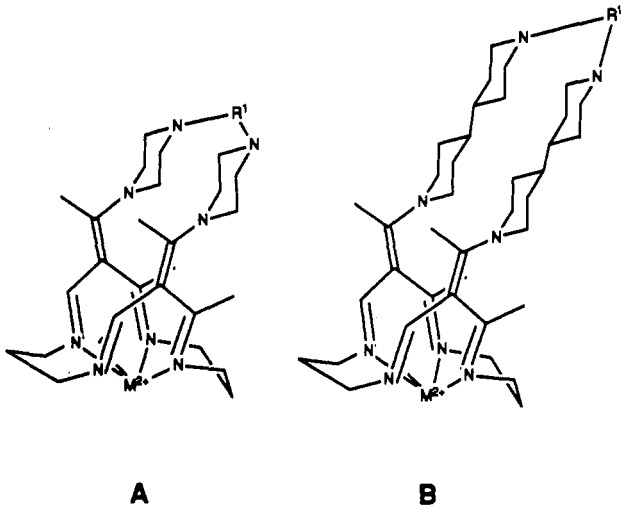

A B

Figure 1. Three-dimensional representations of (a) vaulted cyclidene and (b) supervaulted cyclidene.

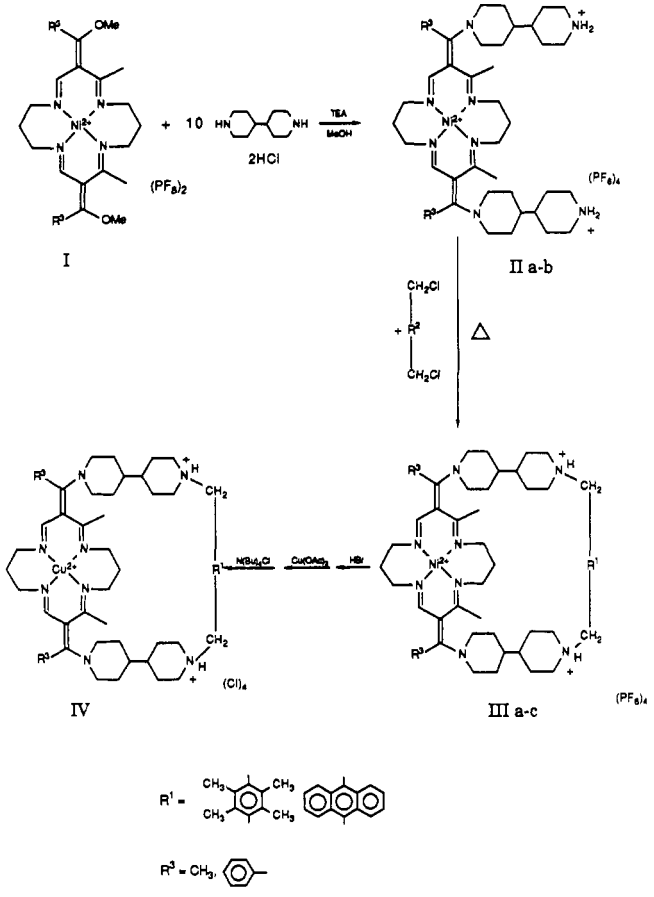

Figure 2. Synthetic scheme for the supervaulted Ni^{2+} and Cu^{2+} cyclidenes: Ia, R^3 = Me; Ib, R^3 = Ph; IIa, R^3 = Me; IIb, R^3 = Ph; IIIa, R^1 = 3,6-durene, R^3 = Me; IIIb, R^1 = 9,10-anthracene, R^3 = Me; IIIc, R^1 = 3,6-durene, R^3= Ph, IV, R^1 = 3,6-durene, R^3 = Me.

complexes of the vaulted cyclidene ligands facilitated the study of inclusion complex formation in greater detail by NMR relaxation techniques.[8,9] The application of the simplified dipolar form of the Solomon–Bloembergen equation[10] to these systems was experimentally justified and subsequently used to calculate distances from the coordinated Cu(II) atom within the cyclidene host to the protons of the hydrophobically bound guest, using spin–lattice relaxation data. These results confirmed the regiospecific binding of small organic guests within the cavity of the host, and the indicated position of the guest showed that enough room remained in the pocket to accommodate a coordinated dioxygen molecule. The first vaulted cyclidene complexes displayed shape selectivity in favor of small rod-shaped molecules, such as alcohols. Association was observed for some methyl-substituted phenols, but the aromatic ring is too large to enter the void within the host.[9]

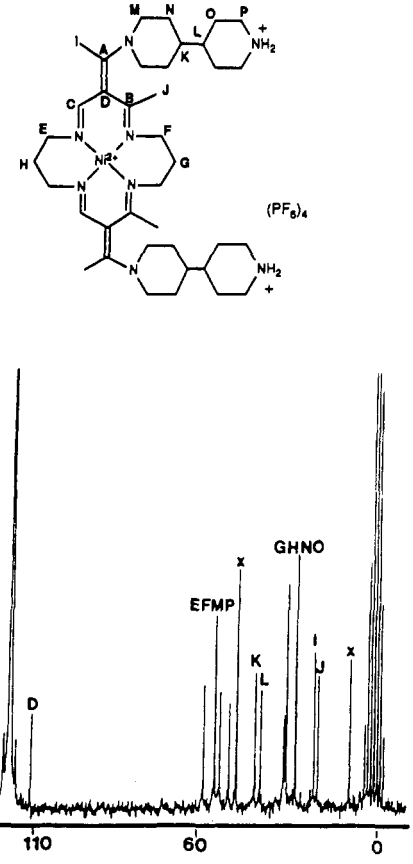

Figure 3. ^{13}C NMR spectrum of [Ni{Me_2(bipiperidiniumyl)$_2$[16]-cyclidene}]$(PF_6)_4$.

The ligand has been redesigned in order to increase the size of the cavity and facilitate the accommodation of larger, perhaps more interesting molecular species as guests. The new "supervaulted" cyclidene ligands use 4,4′-bipiperidine risers, the parent cyclidene macrocycle, and an aromatic ring as a roof (Figure 2). X-ray crystallography confirms the presence of the expected large cavity, and NMR relaxation experiments[10] indicate that substituted phenols are regiospecifically enveloped by the supervault cavity, with the OH group remaining embedded in the solvent sheath. Further, it is clear that a vacant coordination site on the metal remains available for binding dioxygen in the guest–host complex.

Results

Synthesis and Characterization. The nickel(II) and copper(II) supervaulted complexes (Figure 2) are first isolated as tetrakis(hexafluorophosphate) salts, which are metathesized to chloride salts after the nickel(II) has been replaced by copper(II). The chloride salts provides the water solubility required for hydrophobically driven inclusion complex formation. The amines adjacent to the bridging group (Figure 2) are protonated in the supervaulted complexes that have been isolated and characterized. The nickel(II) complexes of the intermediates and bridged supervaulted complexes were characterized by elemental analysis and electrochemistry and by carbon-13 NMR, proton NMR, and infrared spectroscopy.

The carbon-13 NMR spectrum of intermediate II in Figure 2, is shown in Figure 3. Assignments are based on the results of earlier ^{13}C enrichment, off-resonance, and 3D studies on lacunar and vaulted cyclidene complexes.[7,11,12] The NMR spectra confirm

(9) (a) Meade, T. J.; Kwik, W.-L.; Herron, N.; Alcock, N.; Busch, D. H. *J. Am. Chem. Soc.* **1986**, *108*, 1954. (b) Meade, T. J.; Takeuchi, K. J.; Busch, D. H. *J. Am. Chem. Soc.* **1987**, *109*, 725.

(10) Mildvan, A. S.; Gupta, R. K. *Methods Enzymol.* **1978**, *49*, 322.

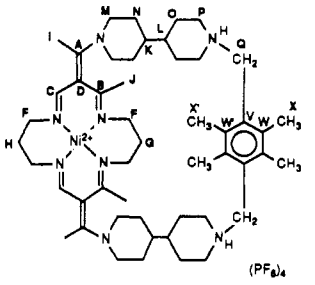

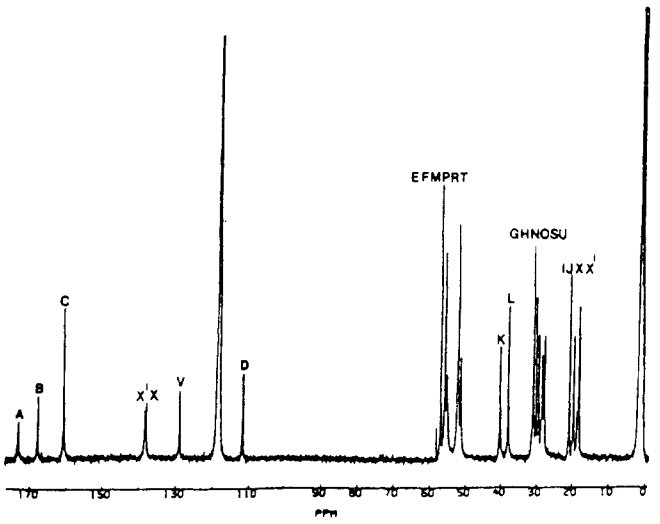

Figure 4. ^{13}C NMR spectrum of [Ni{Me_2(bipiperidiniumyl)$_2$3,6-dur[16]cyclidene}]$(PF_6)_4$.

Table I. Carbon-13 NMR Data for [Ni{supervault[16]cyclidene}]$[PF_6]_4$ in CD_3CN

R^1	R^3	chem shift, ppm
unbridged		172.3, 167.8, 160.1, 111.4, 56,4, 52.8, 51.2, 48.2, 45.7, 39.7, 38.0, 30.3, 29.6, 26.6, 20.6, 19.3
3-6-durene	methyl	172.9, 167.6, 160.5, 138.1, 137.7, 128.7, 111.3, 56.9, 56.6, 55.3, 54.8, 51.8, 51.1, 48.2, 40.0, 37.7, 30.7, 30.0, 29.3, 28.3, 27.5, 20.6, 19.4, 17.9
9,10-anthracene	methyl	172.4, 166.9, 161.2, 133.3, 132.9, 132.1, 127.8, 127.1, 126.9, 56.7, 56.2, 55.5, 55.0, 54.9, 51.6, 40.2, 37.9, 31.9, 30.9, 30.2, 29.9, 29.4, 28.4, 20.5, 18.9, 17.8
3-6-durene	C_6H_5	173.8, 168.4, 162.9, 137.2, 136.5, 134.5, 132.9, 131.5, 130.9, 130.4, 130.1, 113.5, 56.7, 55.7, 55.3, 54.6, 54.3, 53.0, 51.7, 40.4, 39.1, 31.5, 30.7, 30.5, 29.7, 29.2, 28.7, 21.0, 18.1, 17.8

[a] Relative to the 118.2 (br) ppm signal of the solvent.

that II possesses mirror symmetry. Further, carbon atoms M, P, N, and O on the 4,4'-bipiperidine riser (Figure 3) are equivalent pairs, indicating free rotation about the bond between carbon atom A and the adjacent nitrogen atom. This is consistent with results obtained on other species having similar structures.[6] The carbon-13 NMR spectrum of supervaulted complex III is shown in Figure 4. With the addition of the bridge, the rotation of the bipiperidine rings is stopped, and the pairwise equivalence of carbon atoms M, P, N, and O vanishes, increasing the number of peaks in the region between 57 and 25 ppm (Table I). The

Table II. Bond Lengths (Å) for [Ni{Me_2(bipiperidiniumyl)$_2$3,6-dur[16]cyclidene}]$[PF_6]_4$·2C_6H_5CN

Ni–N1	1.185 (25)	Ni–N2	1.891 (23)
Ni–N3	1.860 (28)	Ni–N4	1.885 (25)
N1–C2	1.306 (35)	N1–C14	1.506 (29)
N2–C4	1.230 (41)	N2–C5	1.507 (48)
N3–C7	1.499 (48)	N3–C8	1.291 (39)
N4–C10	1.373 (43)	N4–C12	1.508 (36)
N5–C15	1.347 (41)	N5–C17	1.471 (35)
N5–C21	1.495 (38)	N6–C24	1.502 (44)
N6–C25	1.497 (34)	N6–C27	1.481 (33)
N7–C38	1.514 (40)	N7–C39	1.377 (51)
N7–C43	1.500 (42)	N8–C46	1.518 (55)
N8–C47	1.482 (53)	N8–C49	1.235 (56)
C1–C2	1.559 (45)	C2–C3	1.450 (35)
C3–C4	1.478 (47)	C3–C15	1.438 (37)
C62–C5	1.533 (130)	C62–C61	1.503 (109)
C62–C7	1.881 (108)	C8–C9	1.404 (48)
C9–C10	1.494 (45)	C9–C49	1.458 (49)
C10–C11	1.472 (47)	C12–C13	1.491 (45)
C13–C14	1.580 (40)	C15–C16	1.488 (37)
C17–C18	1.507 (35)	C18–C19	1.564 (43)
C19–C20	1.575 (38)	C19–C22	1.481 (34)
C20–C21	1.467 (36)	C22–C23	1.538 (39)
C22–C26	1.475 (46)	C23–C24	1.443 (40)
C25–C26	1.530 (41)	C27–C28	1.505 (43)
C28–C29	1.389 (46)	C28–C36	1.411 (50)
C29–C30	1.561 (51)	C29–C31	1.449 (45)
C31–C32	1.554 (47)	C31–C33	1.387 (49)
C33–C34	1.440 (38)	C33–C38	1.471 (44)
C34–C35	1.503 (45)	C34–C36	1.406 (40)
C36–C37	1.523 (39)	C39–C40	1.464 (48)
C40–C41	1.534 (47)	C41–C42	1.488 (50)
C41–C44	1.477 (45)	C42–C43	1.498 (43)
C44–C45	1.506 (57)	C44–C48	1.657 (42)
C45–C46	1.482 (55)	C47–C48	1.599 (41)
C49–C50	1.600 (60)		

expected peak attributable to the methylene of the bridging durene, Q, is difficult to see in Figure 4, but has been identified at 57.7 ppm. The carbon atoms K and L are unique, and the proton-coupled spectrum of III reveals their positions (Figure 5, Table I). The resonances at 40 and 37.7 ppm are split into doublets, indicating the single proton on each. Even at 500 MHz, the proton-coupled signals of the other carbon atoms are too complicated to address; however, sufficient peaks are present to indicate the methylene character of each carbon resonance found in the region from 57 to 48 ppm and from 31 to 26 ppm.

X-ray Structure Determination for [Ni{Me_2(bipiperidiniumyl)$_2$-3,6-dur[16]cyclidene}]$(PF_6)_4$·2PhCN. The structure of the supervaulted complex (Figure 6) shows that the design goals of the new cyclidene complexes have been achieved. The floor of the cavity consists of the metal atom and N1, N2, N3, and N4 and has a square planar arrangement with all four Ni–N distances within 0.07 Å of 1.89 Å and N–Ni–N angles within 4° of 90° (Tables II and III). The cyclidene macrocycle assumes the saddle shape that is typical of this class of ligand in its complexes.[13] The overall shape of the cavity resembles that of the vaulted complexes except that the distance from the NiN_4 plane to the center of the durene plane has increased from 8.35 to 12.84 Å, confirming the presence of a large cavity for host–guest association. The width of the cavity varies with height. At the bottom C1–C9, C15–C49, and N5–N8 distances of 5.59, 7.39, and 7.50 Å, respectively, are typical of a rather wide and flat cyclidene macrocycle.[14] The bipiperidine nitrogens furthest from the metal atom are 6.06 Å apart.

The rings of the bipiperidine moieties are pivoted inward about their N···N axes. For the lower rings, the rotation is about 68°, and for the upper ones, it is about 71°. A rotation of 0° would maximize the void between them, while one of 90° for each ring

(11) Busch, D. H.; Olszanski, D. S.; Stevens, J. C.; Schammel, W. P.; Kojima, M.; Herron, N.; Zimmer, L. L.; Holter, K. A.; Mocak, J. *J. Am. Chem. Soc.* **1981**, *103*, 1472.
(12) Meade, T. J.; Fendrick, C. M.; Padolik, P. A.; Cottrell, C. E.; Busch, D. H. *Inorg. Chem.* **1987**, *26*, 4252.
(13) Alcock, N. W.; Lin, W.-K.; Jircitano, A.; Mokren, J. D.; Corfield, P. W. R.; Johnson, G.; Movotnak, G.; Cairns, C. J.; Busch, D. H. *Inorg. Chem.* **1987**, *27*, 440.
(14) Alcock, N. W.; Lin, W.-K.; Cairns, C.; Pike, G. A.; Busch, D. H. *J. Am. Chem. Soc.* **1989**, *111*, 6630.

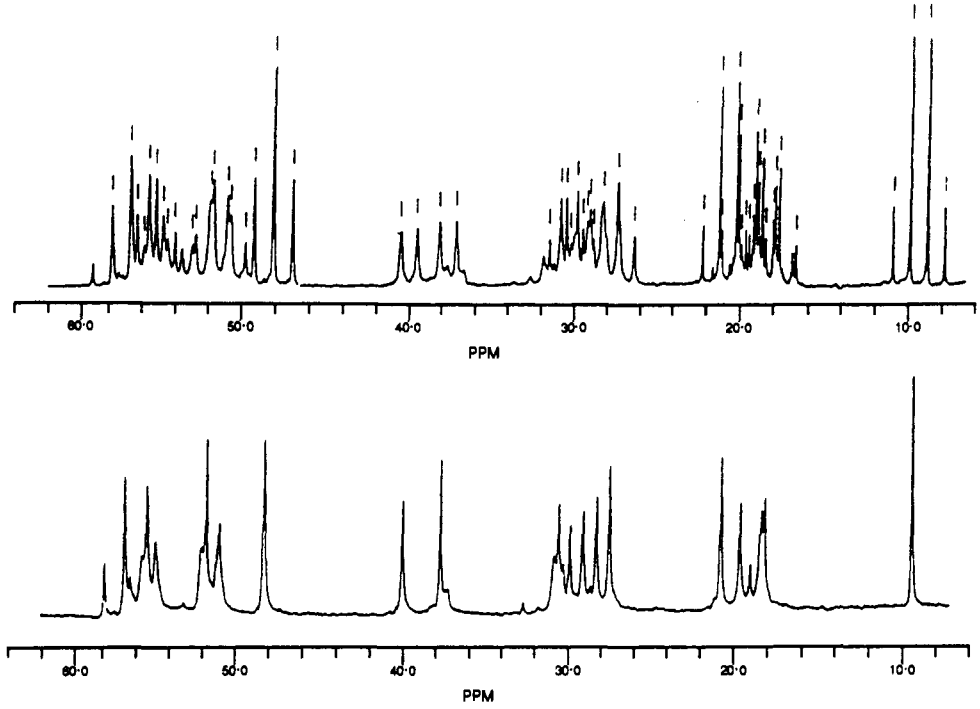

Figure 5. ^{13}C NMR proton-coupled spectrum of $[Ni\{Me_2(bipiperidiniumyl)_2$3,6-dur[16]cyclidene$\}](PF_6)_4$.

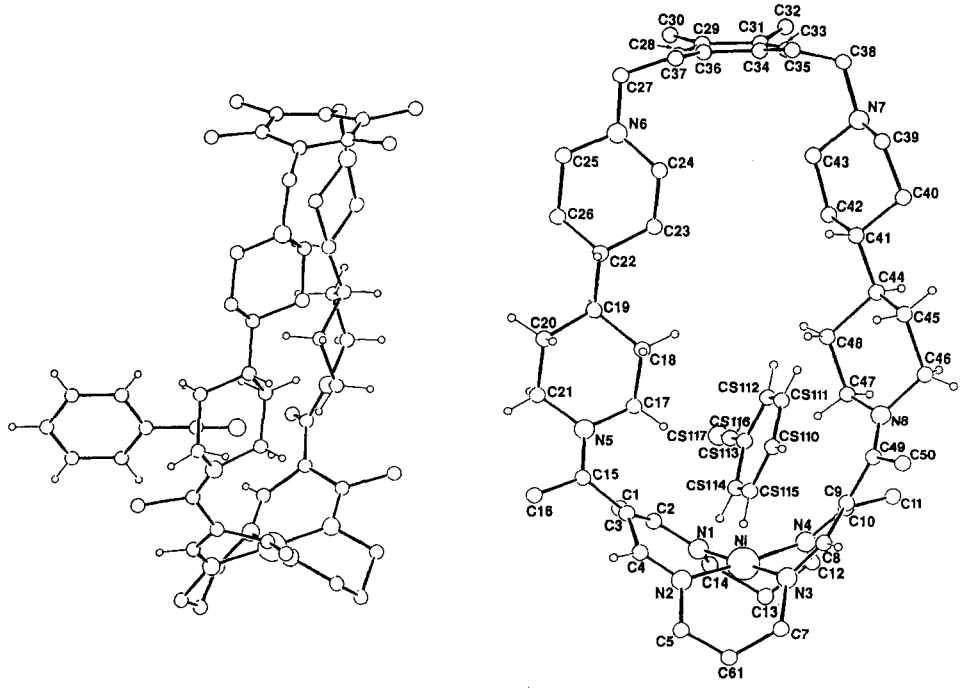

Figure 6. Two views of the "supervault" durene complex, cation IIIa, giving the atomic numbering and showing the interaction with one of the solvent benzonitrile molecules. Only the major position for C6 is included (C61), and the H atoms on this part of the macrocycles are omitted. Hydrogen atoms that are included have artificially low temperature factors.

would result in the rings being edge-to-edge, essentially filling the cavity. The rings have therefore pivoted so that the inner protons of the bipiperidine are directed toward the interior of the void.

One prominent feature of the structure is the evidence of strain in the durene cap. This can clearly be seen in Figure 6, in the displacements of the CH_3 groups outward from the cavity and of the 3,6-position ring carbons (C28, C33) inward.

A benzonitrile molecule is located partially in the cavity (Figure 6) with the nitrogen end directed into the void.[15] A second benzonitrile molecule occupies an uninteresting space between molecules (see Figure 7). The partially encapsulated benzonitrile molecule may have affected the pivoting of the bipiperidine rings in order to maximize interactions between the benzonitrile nitrogen and the protons of the bipiperidine rings.[6,15] In a polar solvent such as water, however, the orientation of the guest would be expected to be reversed. The hydrophobic ring of benzonitrile should occupy the hydrophobic environment, and the polar nitrogen should associate with the solvent water.

Proton NMR Relaxation Studies. Tables IV–VI and Figures 11–14 present data on the relaxation of guest protons due to complexation with the host molecule.

Discussion

Design Considerations. An essential design feature of the vaulted cyclidene complexes developed by Takeuchi[6] is a large

(15) In the vaulted anthracene structure, an acetonitrile molecule was found to be internally associated within the confines of the void.[6] The nitrogen atom of acetonitrile is within 2.97 Å of the protons of the piperazine rings while its methyl group is directed away from the cavity.

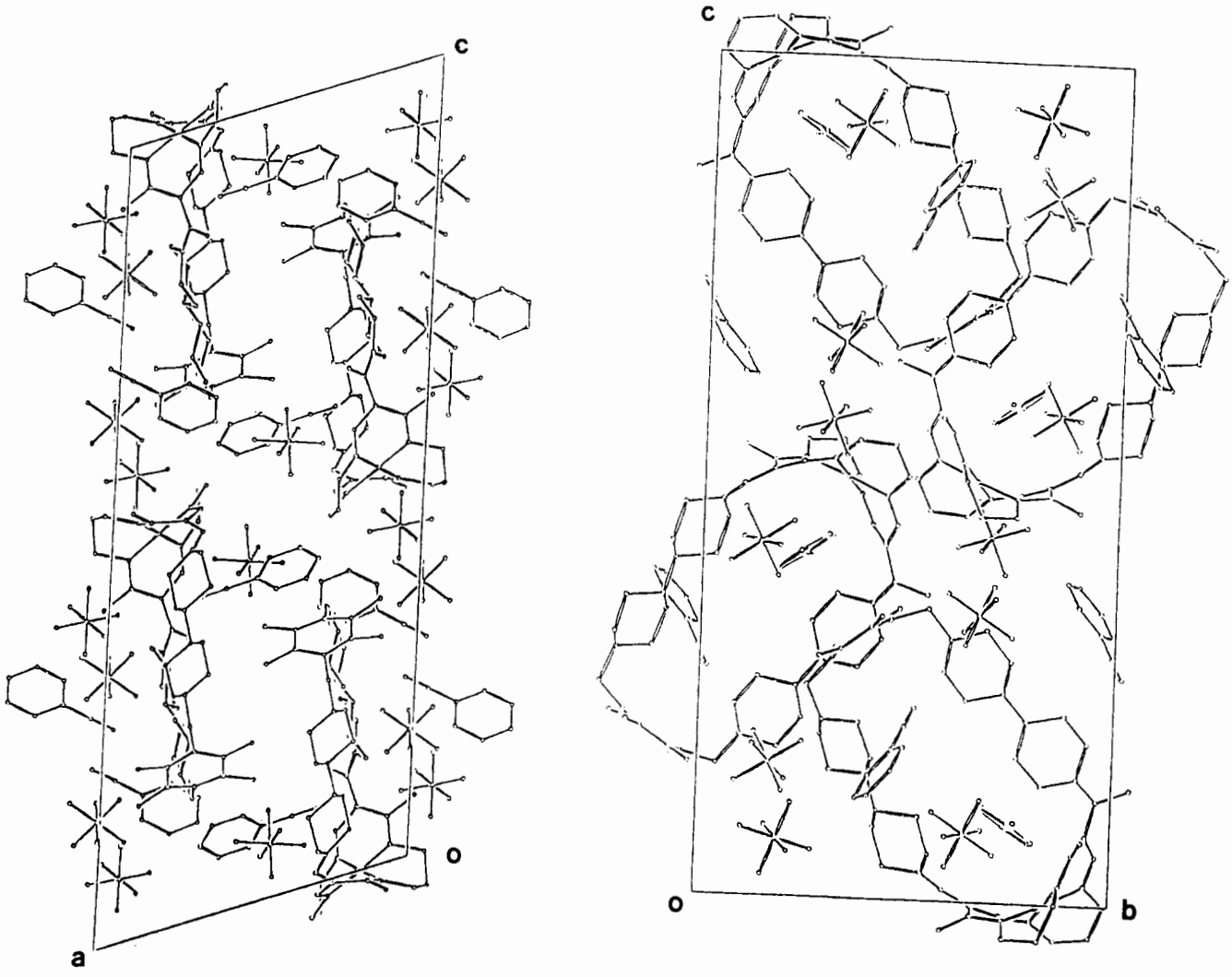

Figure 7. Packing diagrams for IIIa, viewed down the *b* (left) and *a* (right) axes.

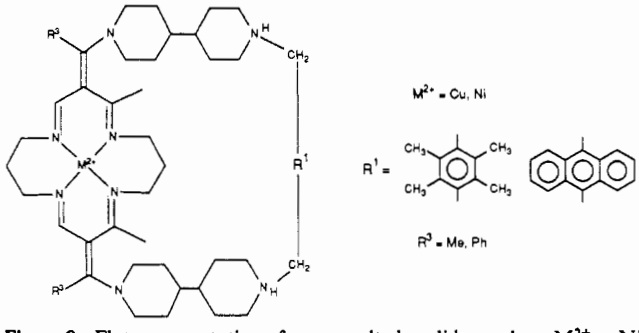

Figure 8. Flat representation of supervaulted cyclidene where M^{2+} = Ni and Cu, R^1 = 3,6-durene and 9,10-anthracene, and R^3 = Me and Ph.

preformed cavity, in sharp contrast to several classes of organic hosts, including crown ethers, cryptates, and many types of cyclophanes whose cavities are formed during the course of host–guest complexation.[16] In the supervaulted cyclidene structures, as detailed in the results section, the NiN_4 plane functions as the floor of the void, while the 4,4′-bipiperidine risers are the walls and, for example, the durene moiety forms the roof (Figure 8).

Contrary to experience with the vaulted complexes in which the piperidine risers remain unprotonated, the supervaulted complexes were isolated as the salts of doubly protonated cations having an overall 4+ charge. This was clearly revealed by the elemental analysis. The implied protonation of the saturated amine groups of the risers (most distant from metal) was confirmed by electrochemical studies. Scan A of Figure 9 represents the reversible $Ni^{III/II}$ couple of the supervaulted complex. In contrast, the scan for the $Ni^{III/II}$ couple for the vaulted cyclidene complex is highly irreversible, a result that has been interpreted as arising from irreversible oxidation of the distant nitrogen atom of the piperazine ring.[17] Protonation of the vaulted complex results in reversible cyclic voltammetry. This suggests that the reversible behavior of the bipiperidyl derivative is the result of protonation of its nitrogen atoms. This was confirmed by the addition of sodium methoxide; the resulting solution gave an irreversible wave (scan B), which is attributed to the overlap of the irreversible oxidation of the distant nitrogen on the bipiperidine with the $Ni^{III/II}$ couple. Upon addition of HPF_6, a reversible wave is again observed (Figure 9c), indicating that the nitrogen of the bipiperidine is again protonated and that the irreversible oxidation of the amine does not occur.

Replacement of the methyl group at the R^3 position with a phenyl group should enhance the hydrophobicity of the pocket. The synthesis and isolation of the phenyl-substituted product followed the course outlined previously for the vaulted systems.[6,18] The ^{13}C NMR spectrum of $[Ni\{Ph_2$-(bipiperidiniumyl)$_2$3,6-dur-[16]cyclidene$\}](PF_6)_4$ is shown in Figure 10. It may be noted that the number of signals in the 60 to 30 ppm range indicates that every carbon atom is unique and that the bipiperidine rings are not free to rotate.

Inclusion Complex Formation with $[Cu\{Me_2$(bipiperidiniumyl)$_2$3,6-dur[16]cyclidene$\}](Cl)_4$ and Organic Guests. Studies on the paramagnetic contribution to the relaxation rates of protons[19] of the guest molecules, using vaulted cyclidene host

(16) Cram, D. J. *Angewandte Chem.* **1986**, *25*, 1039.

(17) Goldsby, K. A.; Busch, D. H. Unpublished results.
(18) Coltrain, B. K. Ph.D. Thesis, The Ohio State University, 1984.

Table III. Bond Angles (deg) for [Ni{Me_2(bipiperidiniumyl)$_2$3,6-dur[16]cyclidene}][PF_6]$_4$

N1-Ci-N2	67.4 (11)	N1-Ni-N3	177.3 (9)
N2-Ni-N3	90.1 (11)	N1-Ni-N4	94.3 (11)
N2-Ni-N(4)	175.4 (9)	N3-N1-C14	88.1 (12)
Ni-N1-C2	127.9 (17)	Ni-N1-C14	124.1 (17)
C2-N1-C14	107.8 (23)	Ni-N2-C4	123.3 (23)
Ni-N2-C5	120.6 (20)	C4-N2-C5	116.1 (25)
Ni-N3-C7	123.6 (20)	Ni-N3-C8	119.3 (24)
C7-N3-C8	117.1 (29)	Ni-N4-C10	128.2 (20)
Ni-N4-C12	117.8 (19)	C10-N4-C12	113.9 (24)
C15-N5-C17	123.8 (24)	C15-N6-C25	107.8 (24)
C24-N6-C27	117.9 (23)	C25-N6-C27	111.4 (19)
C38-N7-C39	118.7 (24)	C38-N7-C43	112.0 (25)
C39-N7-C43	107.7 (28)	C46-N8-C47	105.6 (35)
C46-N8-C49	127.0 (49)	C47-N8-C49	127.4 (35)
N1-C2-C1	124.0 (21)	N1-C2-C3	118.7 (27)
C1-C2-C3	115.7 (23)	C2-C3-C4	116.4 (23)
C1-C2-C15	128.9 (29)	C4-C3-C15	114.0 (23)
N2-C4-C3	124.5 (25)	N2-C5-C61	115.7 (36)
N2-C5-C62	112.7 (51)	C61-C5-C62	61.3 (50)
C5-H5a-C62	79.2 (43)	C5-C61-C62	63.5 (59)
C62-C61-C7	76.5 (52)	C61-H61b-C62	83.8 (66)
C62-H61b-C7	87.8 (64)	N3-C7-C61	112.0 (41)
N3-C7-C62	105.2 (47)	C61-C7-C62	51.5 (39)
C62-H7a-C7	95.5 (39)	N3-C8-C9	127.2 (33)
C8-C9-C10	121.2 (28)	C8-C9-C49	120.7 (30)
C10-C9-C49	118.1 (32)	N4-C10-C9	111.3 (29)
N4-C10-C11	121.8 (26)	C9-C10-C11	123.1 (31)
N4-C12-C13	111.3 (24)	C12-C13-C14	115.0 (23)
N1-C14-C13	105.4 (22)	N5-C15-C3	115.9 (24)
N5-C15-C16	119.9 (24)	C3-C15-C16	123.7 (26)
N5-C17-C18	111.7 (19)	C17-C18-C19	113.8 (24)
C18-C19-C20	104.6 (24)	C18-C19-C22	115.5 (24)
C20-C19-C22	110.9 (20)	C19-C20-C21	112.3 (20)
N5-C21-C20	115.7 (24)	C19-C22-C23	113.4 (20)
C19-C22-C26	112.6 (25)	C23-C22-C26	106.6 (25)
C22-C23-C24	113.5 (23)	N6-C24-C23	113.5 (27)
N6-C25-C26	111.4 (22)	C22-C26-C25	116.8 (28)
N6-C27-C28	112.4 (22)	C27-C28-C29	117.3 (31)
C27-C28-C36	117.5 (28)	C29-C28-C36	125.2 (30)
C28-C29-C30	123.5 (29)	C28-C29-C31	115.1 (31)
C30-C29-C31	121.3 (26)	C29-C31-C32	113.5 (30)
C29-C31-C33	118.9 (27)	C32-C31-C33	127.1 (29)
C31-C33-C34	123.6 (28)	C31-C33-C38	115.1 (26)
C34-C33-C38	121.0 (30)	C33-C34-C35	119.7 (26)
C33-C34-C36	116.7 (27)	C35-C34-C36	123.6 (24)
C28-C36-C34	117.8 (25)	C28-C36-C37	125.0 (26)
C34-C36-C37	116.7 (23)	N7-C38-C33	116.1 (26)
N7-C39-C40	118.9 (28)	C39-C40-C41	107.7 (29)
C40-C41-C42	110.0 (29)	C40-C41-C44	108.4 (28)
C40-C41-C44	115.5 (25)	C41-C42-C43	112.2 (25)
N7-C43-C42	112.2 (28)	C41-C44-C45	116.6 (27)
C41-C44-C48	111.4 (27)	C45-C44-C48	101.4 (28)
C44-C45-C46	113.0 (29)	N8-C46-C45	113.7 (34)
N8-C47-C48	119.4 (26)	C44-C48-C47	111.8 (24)
N8-C49-C9	122.6 (38)	N8-C49-C50	117.9 (34)
C9-C49-C50	118.8 (35)		

Table IV. Relaxation Times[a] and Calculated Distances for the Guest 2,6-Dimethylphenol (p = 1.07 × 10^{-3})[b] with Host IV

protons	Me	meta	para H
$(T_1)_0$,[c] s	4.23 ± 0.02	9.72 ± 0.01	8.43 ± 0.03
T_1,[d] s	2.78 ± 0.07	1.38 ± 0.18	1.89 ± 0.04
r, Å	6.4 ± 0.2	4.8 ± 0.1	5.2 ± 0.1

[a] Data at ν = 500 MHz and T = 305 K using a Bruker AM-500 spectrometer. [b] [host] = 5.25 × 10^{-5} M; [guest] = 4.91 × 10^{-2} M. [c] Longitudinal relaxation time in the absence of paramagnetic complex. [d] Longitudinal relaxation time in the presence of paramagnetic complex.

complexes, have clearly shown that hydrophobic binding of the guest takes place within the cavities of these cyclidene derivatives.[8,9] A major factor influencing the binding of inclusion complexes involves the match in size and kind between the host and guest.[20,21]

(19) Solomon, I.; Bloembergen, J. *Chem. Phys.* **1956**, *25*, 261.

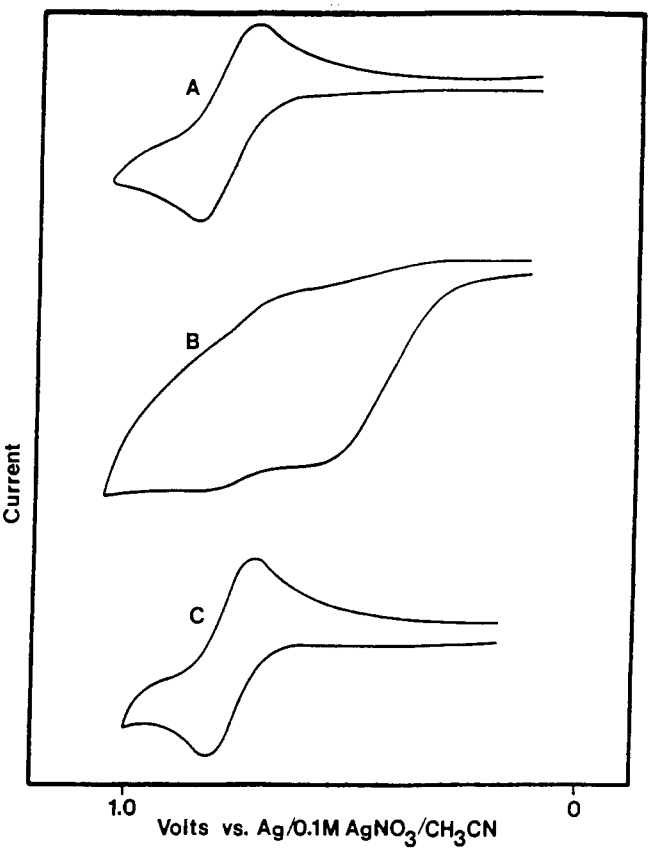

Figure 9. Cyclic voltammogram for the [Ni{Me_2(bipiperidiniumyl)$_2$3,6-dur[16]cyclidene}](PF_6)$_4$ at a Pt wire electrode vs Ag/0.1 M $AgNO_3$/CH_3CN: (a) in 0.1 M TBAT/CH_3CN; (b) following addition of NaOMe; (c) following addition of excess 60% $H^+PF_6^-$.

For hydrophobic binding, an increase in the extent of the hydrophobic host surface encompassing the guest is expected to cause an increase in the binding constant.[22] Earlier studies with the original vaulted cyclidene host showed that the aromatic rings of phenols are not accepted into the void of the host.[9] However, regiospecific binding was observed with inclusion in the void of the methyl substituents on 2,6-dimethyl-, 2,5-dimethyl-, and 3,5-dimethylphenol.

The large cavity of the supervaulted cyclidene complex (host IV) is ideally suited to accommodate relatively large organic guests. The relaxation data and calculated distances for the guest 2,6-dimethylphenol, and host IV are shown in Table IV. The results are consistent with expectation, and the new host readily engulfs the entire phenol molecule (Figure 11). The aromatic ring of the guest lies deeply in the cavity and is oriented parallel to the bipiperidine walls. The phenolic OH group is directed away from the cavity and is so located as to permit solvation. With the previously reported smaller vaulted cyclidene host,[9] the aromatic ring of the phenol lies flat against the cavity entrance, apparently held in place by inclusion of a methyl substituent in the cavity.

Figure 11 was generated by using the computer program named ChemGraph,[23] the atomic coordinates from the crystal structure determination on the host molecule, and the distances derived from the NMR relaxation studies. The distances derived from the NMR data are given in Table IV. They are sixth-power averaged distances for the equivalent protons present in the 2,6-dimethylphenol guest. In addition, the following distances (Å) were used in constructing Figure 11: Cu-H_{meta} = r_A = 4.23, r_B = 7.89, and r_{av} = 4.7; Cu-H_{CH_3}, r_A = 6.114, r_B = 9.50, and r_{av} = 6.7.

(20) Cram, D. J. *J. Inclusion Phen.* **1988**, *6*, 397.
(21) Lehn, J.-M. *J. Inclusion Phen.* **1988**, *6*, 351.
(22) Meade, T. J.; Busch, D. H. *Prog. Inorg. Chem.* **1985**, *33*, 59.
(23) ChemGraph: Chemical Design Ltd., Oxford England, (0865) 251483, 1984. This figure was prepared by Dr. Norman Herron; we appreciate his contribution.

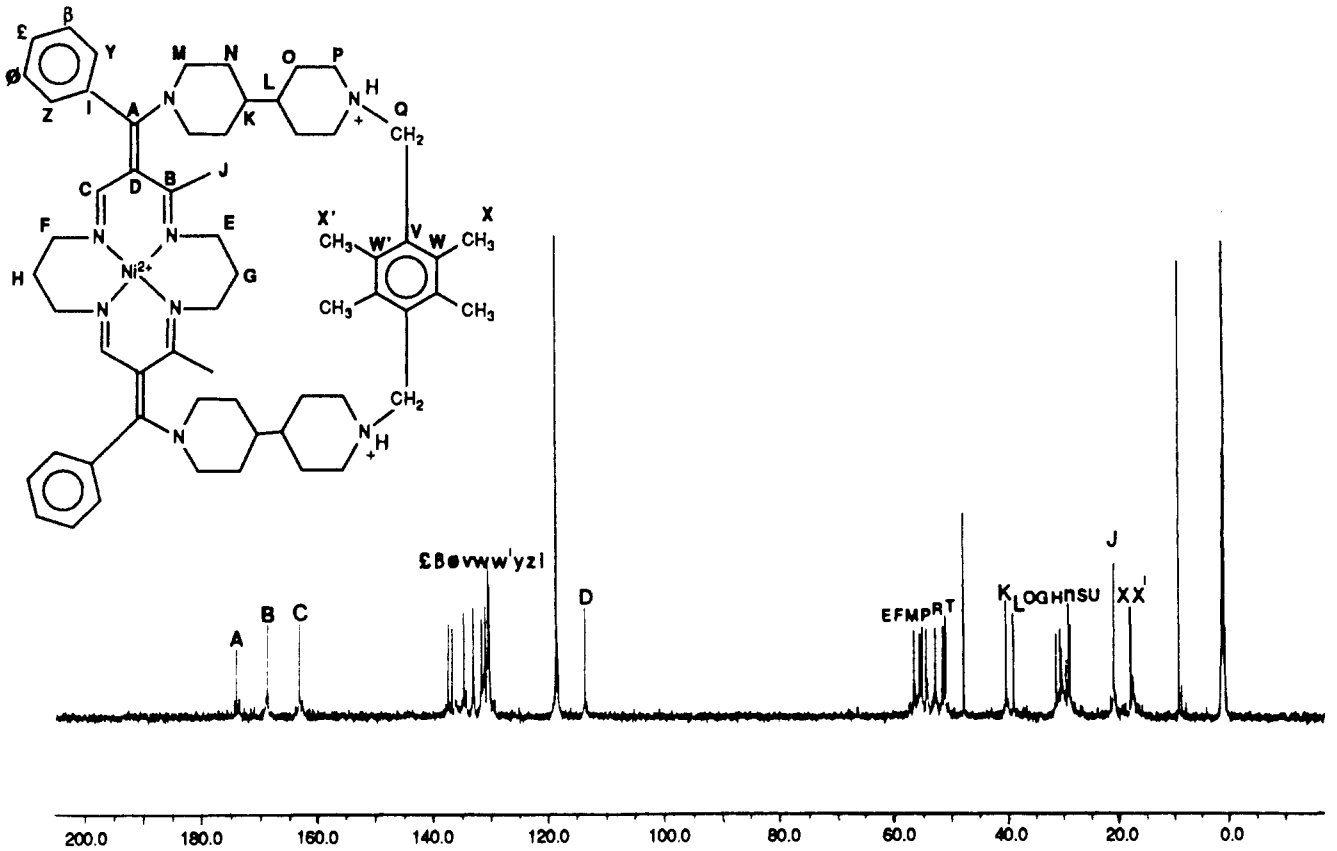

Figure 10. ^{13}C NMR spectrum of [Ni{Ph_2(bipiperidiniumyl)$_2$3,6-dur[16]cyclidene}]$(PF_6)_4$.

Table V. Relaxation Times[a] and Calculated Distances for the Guest 2-(3-Methylphenyl)ethanol and Host IV

	α(CH_2)	β(CH_2)	meta H	methyl	ortho H
$(T_1)_0$, s	2.63 ± 0.02	2.38 ± 0.01	6.88 ± 0.07	4.41 ± 0.02	7.27 ± 0.01
T_1, s	2.22 ± 0.04	1.96 ± 0.05	2.94 ± 0.14	2.07 ± 0.05	4.28 ± 0.09
r, Å	6.9 ± 0.1	6.6 ± 0.1	5.8 ± 0.2	5.6 ± 0.2	6.5 ± 0.1

[a] ν = 500 MHz; T = 304 K; [host] = 5.25 × 10^{-5} M, [guest] = 5.50 × 10^{-2} M.

Table VI. Relaxation Times[a] and Calculated Distances for the Guest *n*-Butanol (p = 9.60 × 10^{-4})[b] and Host IV

	α-H	β-H	γ-H	δ-H
$(T_1)_0$, s	6.19 ± 0.03	5.47 ± 0.06	5.86 ± 0.01	6.11 ± 0.02
T_1, s	5.44 ± 0.08	4.59 ± 0.15	4.76 ± 0.09	3.87 ± 0.06
r, Å	8.3 ± 0.1	7.7 ± 0.1	7.5 ± 0.1	6.5 ± 0.1

[a] ν = 500 MHz; T = 304 K. [b] [host] = 5.25 × 10^{-5} M, [guest] = 5.49 × 10^{-2} M.

Figure 11a provides a space-filling representation of the structure, while parts b and c of Figure 11 make it easy to distinguish between the host and guest by successively reducing each of them to stick representations. Figure 11d–f gives corresponding side views of this inclusion complex. This molecular image promotes the view that the guest molecule is immersed in the cavity of the supervaulted host and indicates that the host–guest complex is circumscribed by a fairly smooth perimeter that may be taken as modeling the solvent sheath. Further, the OH group clearly protrudes into the solvent sheath, permitting solvation of that polar group and providing the driving force for the regiospecific binding. Finally, the lower halves of the bipiperidine rings have rotated into parallel orientations to accommodate the guest.

Characterization in the solid state of guest–host complexes of the kind described here would be highly desirable. However, all attempts to isolate such solid materials with phenols as guests have failed. The structure determination reported here actually involves benzonitrile solvent molecules, one of which behaves as a rather different guest molecule. Figure 6 shows that, in the hydrophobic environment of the crystal lattice, the polar nitrile function projects into the cavity. As detailed with respect to an earlier structure in which an acetonitrile molecule performed analogously,[6] specific van der Waals interactions with hydrogen atoms of the host are responsible for this orientation. The behavior of the same host–guest pair in highly polar hydrogen-bonding aqueous media is expected to be entirely different.

Figure 12 is included to contrast the behavior of host IV with respect to guest molecules in the hydrophobic solid state with the hydrophillic aqueous solution state. In the solid state, a benzonitrile molecule is so oriented that the polar group points into the cavity and is nearest the metal, but still much too far away for bonding. In contrast, as Figure 11 shows, in aqueous solution the apolar aromatic moiety is contained in the cavity with the polar OH group projecting out into the solvent.

The results of measurements using host IV and 2-(3-methylphenyl)ethyl alcohol as the guest are presented in Table V. The protons adjacent to the OH group (α) are most distant from the Cu(II) center, while the β protons are the next furthest away. It appears that the methyl group and the meta proton are approximately the same distance from the metal center. This result may be rationalized in terms of an averaging of the orientation of the 2-(3-methylphenyl)ethyl alcohol guest as it approaches and enters the cavity.

Another interesting observation on the host IV–2-(3-methylphenyl)ethanol interaction may be seen from a stack plot of spectra of the guest itself (Figure 13). The T_1 values of the different protons in the region of 7.0 ppm are sufficiently different to resolve a set of previously overlapping signals (Figure 14). In Figure 14, the top spectrum is that for a normal pulse width of 4 μs. The lower spectrum is that for a 5-s delay value from Figure 13, using the inversion recovery delay 180°, τ, 90° pulse sequence. The signal due to the two protons appears as a triplet during normal

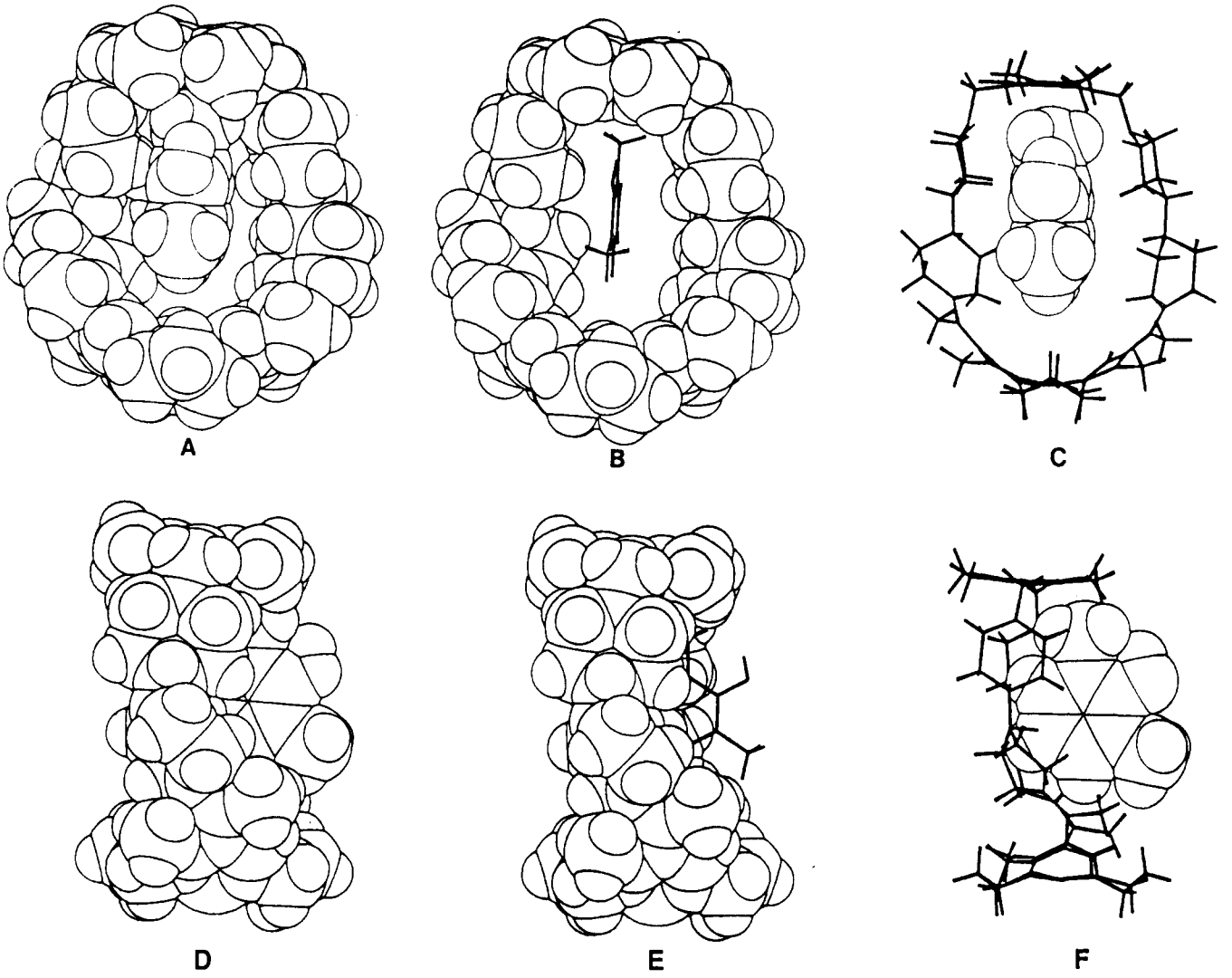

Figure 11. Various depictions of the inclusion complex between host III and the 2,6-dimethylphenol guest.

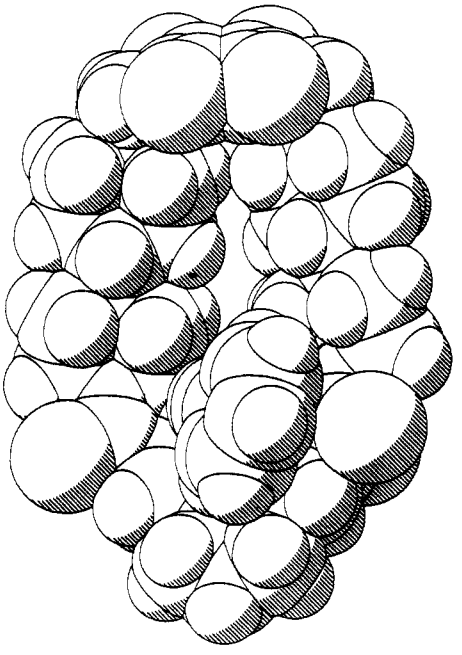

Figure 12. Spacefilling representation of the actual structure of the complex in Figure 6.

data acquisition; the signal is due to the para and ortho protons of the benzene ring. However, when the appropriate delay value is used, the triplet is resolved into the expected set of two doublets.

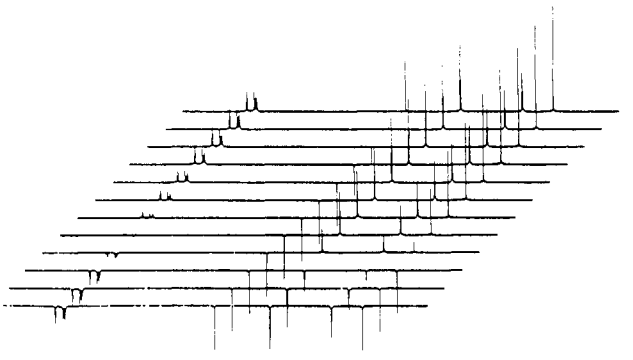

Figure 13. Stack plot of the inversion recovery sequence for the guest 2-(3-methylphenyl) ethanol.

The remarkable difference in the respective T_1 values for the two protons is obvious from the recovery of the signal at higher field, while the lower field signal remains inverted.

For comparison with earlier studies, the relaxation data for *n*-butanol as the guest with host IV is presented in Table VI. The distances calculated for this guest are remarkably similar to those obtained with the smaller vaulted host complex.[8] An identical regiospecific behavior is observed with the methyl group protruding into the cavity while the protons adjacent to the OH group indicate that the hydroxyl function is sticking out into the solvent. This congruent behavior for the two very different hosts suggests that the guest has found similar sites in the two systems. In turn, this suggests that, in the case of the larger host IV, the lower half of the bipiperidine ring system may imitate the conformation of the

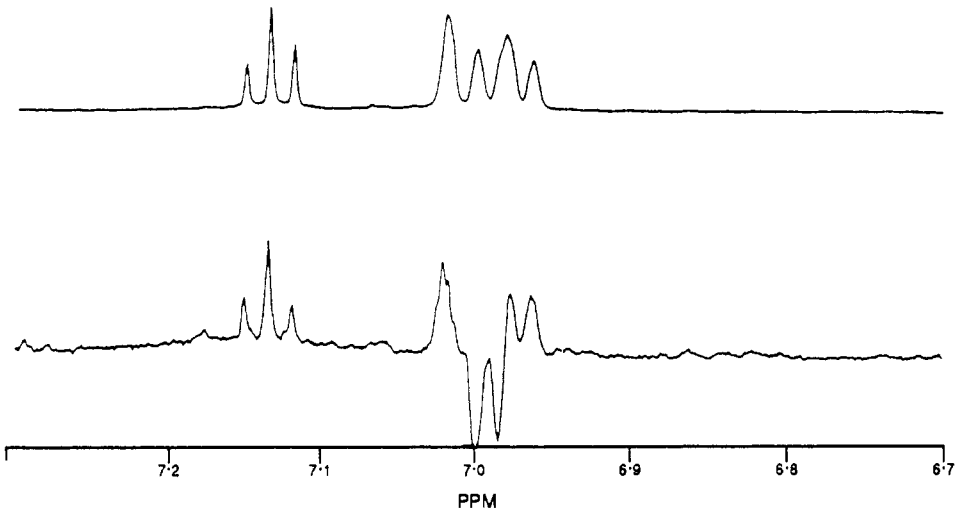

Figure 14. ^1H spectra of the guest 2-(3-methylphenyl) ethanol. Top spectrum: normal acquisition with a 4-s pulse width. Bottom spectrum: 5-s delay scan from an inversion recovery pulse sequence.

smaller host III in order to accommodate the smaller guest.

Conclusions

The supervaulted complexes reported here represent a substantial advance in the use of inclusion complexes as part of an ongoing effort in the design of enzyme mimics. Crystallographic data have confirmed the expanded cavity size and the nature of the supervaulted hosts. The dimensions of the transition-metal host are suitable for the binding of organic substrates containing aromatic rings. An experimentally justified NMR relaxation technique for the determination of the precise nature of the host–guest complexation has been successfully applied to these new complexes. Phenol guests are completely engulfed in the supervaulted complexes while they are only partially enclosed by the vaulted complexes.

Experimental Section

Materials. Solvents and reagents used in the synthesis of nickel(II) and copper(II) complexes were of reagent grade and used without further purification.

Synthesis of Nickel(II) Supervaulted Cyclidene Complexes. [(2,12-Dimethyl-3,11-bis[1-(4,4′-bipiperidin-1′-ium-1-yl)ethylidene]-1,5,9,13-tetraazacyclohexadeca-1,4,9,12-tetraene-κ^4N)nickel(II)] Tetrakis(hexafluorophosphate), [Ni{Me_2(bipiperidiniumyl)$_2$[16]cyclidene}]$(PF_6)_4$. Five grams of [Ni{$Me_2(MeO)_2$[16]cyclidene}]$(PF_6)_2$ was dissolved in 250 mL of acetonitrile and added dropwise over a period of 4 h to a solution of 16.4 g of 4,4′-bipiperidine dihydrochloride and 18.9 mL of triethylamine in 700 mL of methanol. The reaction was allowed to proceed for an additional 2 h with constant stirring. The volume of the solution was reduced to approximately 150 mL, and excess 4,4′-bipiperidine (confirmed via ^{13}C) was filtered off and discarded. The solution was reduced in volume to an oil and redissolved in 100 mL of acetonitrile, and a solution of excess ammonium hexafluorophosphate in ethanol was added. The mixture was allowed to stand overnight in a refrigerator, and the solid that appeared was filtered and discarded. The solution was reduced in volume to approximately 10 mL and passed through a neutral alumina column with a 10% methanol/acetonitrile (v/v) solution as the eluent. The solution was reduced in volume to an oil and dissolved in 50 mL of methanol. To the methanol solution of the product was added 50 mL of water, and the voluminous yellow precipitate that immediately formed was collected and dried in vacuo. Yield: 2.1 g, 50%. Anal. Calcd for $NiC_{38}H_{62}N_8(PF_6)_4$: C, 35.39; H, 5.17; N, 8.69; Ni, 4.55. Found: C, 35.46; H, 5.31; N, 8.91; Ni, 4.67. When the isolation of this intermediate is not necessary, the following abbreviated procedure is appropriate.

Once the reaction described above is completed (~6 h) the reaction mixture is reduced in volume to dryness, dissolved in a minimum of acetonitrile, and filtered. This dark red solution may then be used to proceed directly to the subsequent bridging reaction described below.

**[(18,25-Dihydro-2,8,10,21,22,33,41,42-octamethyl-3,7,11,18,25,32,35,39-octaazaheptacyclo[24.7.7.2^{20,23}.2^{11,14}.2^{15,18}.2^{25,28}.2^{29,32}]pentaconta-2,7,9,20,22,33,34,39,41-nonaene-κ^4N)nickel(II)] Tetrakis(hexafluorophosphate), [Ni{Me_2(bipiperidiniumyl)$_2$3,6-dur[16]cyclidene}]$(PF_6)_4$.** The solution of [Ni{(bipiperidiniumyl)$_2Me_2$[16]-cyclidene}]$(PF_6)_4$ in 250 mL of acetonitrile was placed in a 250-mL pressure-equalizing funnel along with 1.28 g of triethylamine. In a second 250-mL pressure-equalizing funnel was placed 0.8 g (3.8 mmol) of 3,6-bis(chloromethyl)durene in 250 mL of acetonitrile. Both were dropped simultaneously over a period of 3 h into a 1000-mL three-neck round-bottom flask containing 300 mL of boiling acetonitrile. The reaction was refluxed for an additional 3 h and was then reduced in volume, filtered, and passed down a neutral alumina column, and the fastest moving yellowish band was collected. (It is frequently necessary to repeat the column step.) A solution of 2 g of ammonium hexafluorophosphate was dissolved in 50 mL of ethanol and added slowly to the orange solution obtained from the alumina column. The solution was reduced to dryness and slurried in 100 mL of a solution 50/50 methanol/water (v/v), filtered, and dried in vacuo. The yellow-orange solid was recrystallized from an acetonitrile/ethanol solution. X-ray quality crystals were obtained by a further recrystallization from benzonitrile. Anal. Calcd for $NiC_{50}H_{80}N_8(PF_6)_4 \cdot CH_3CN$: C, 42.39; H, 5.71; N, 7.61; Ni, 3.98. Found: C, 42.13; H, 6.00; N, 7.82; Ni, 3.65.

[(18,29-Dihydro-2,8,10,37-tetramethyl-3,7,11,18,29,36,39,43-octaazanonacyclo[28.7.7.6^{20,27}.2^{11,14}.2^{15,18}.2^{29,32}.2^{33,36}.0^{21,26}.0^{25,50}]octapentaconta-2,7,9,20(50),21,23,25,27(45),37(1),38,43,46,48-triecaene-κ^4N]nickel(II)] Tetrakis(hexafluorophosphate), [Ni{Me_2(bipiperidiniumyl)$_2$9,10-anthra-[16]cyclidene}]$(PF_6)_4$. This reaction was performed in the same manner as the preceding reaction with the substitution of 0.5 g 9,10-bis(chloromethyl)anthracene and by allowing the reaction to proceed an additional 8 h at reflux. Anal. Calcd for $NiC_{54}H_{78}N_8(PF_6)_4 \cdot 2CH_3CN$: C, 42.70; H, 5.19; N, 7.38; Ni, 3.86. Found: C, 42.48; H, 5.01; N, 7.30; Ni, 3.66.

Synthesis of R^3 = Phenyl, Supervaulted Cyclidene Complexes. [(2,12-Dimethyl-3,11-bis[1-(4,4′-bipiperidin-1′-ium-1-yl)benzylidene]-1,5,9,13-tetraazacyclohexadeca-1,4,9,12-tetraene-κ^7N)nickel(II)] Tetrakis(hexafluorophosphate), [Ni{Ph_2(bipiperidiniumyl)$_2$[16]cyclidene}]$(PF_6)_4$. A solution of 6.0 g of [Ni{$Ph_2(MeO)_2$[16]cyclidene}]$(PF_6)_2$ was dissolved in 250 mL of acetonitrile and added dropwise over a period of 4 h to a solution of 17.2 g of 4,4′-bipiperidine dihydrochloride and 21 mL of triethylamine in 600 mL of methanol. The reaction mixture was reduced in volume to approximately 50 mL and filtered. No analytical data were acquired.

**[(18,25-Dihydro-2,8,10,21,22,33,41,42-octamethyl-10,33-diphenyl-3,7,11,18,25,32,39-octaazaheptacyclo[24.7.7.2^{20,23}.2^{11,14}.2^{15,18}.2^{25,28}.2^{29,32}]pentaconta-2,7,9,20,22,33,34,39,41-nonaene-κ^4N)nickel(II)] Tetrakis(hexafluorophosphate), [Ni{Ph_2(bipiperidiniumyl)$_2$3,6-dur[16]-cyclidene}]$(PF_6)_4$.** A solution of [Ni{Ph_2(bipiperidiniumyl)$_2$[16]-cyclidene}]$(PF_6)_4$ in 200 mL of acetonitrile and 0.8 g of 3,6-bis(chloromethyl)durene in 200 mL of acetonitrile were dropped simultaneously into a boiling reservoir of 200 mL of acetonitrile over a period of approximately 3 h. The reaction mixture was allowed to react for an additional 8 h before cooling to room temperature. The volume of the solution was reduced to about 15 mL, filtered, and passed through a neutral alumina column using acetonitrile as the eluent, and the fastest moving yellow band was collected. A solution of excess NH_4PF_6 in ethanol was added to the solution, and the resulting solution was rotary evaporated to a reddish orange oil. The oil was slurried in a 20% methanol/water (v/v) solution and, after 24 h, was filtered and dried in vacuo. The solid was recrystallized from an ethanol/acetonitrile solution.

Synthesis of Cu(II) Complexes. [(18,25-Dihydro-2,8,10,21,22,33,41,42-octamethyl-3,7,11,18,25,32,35,39-octaazaheptacyclo[24.7.7.2^{20,23}.2^{11,14}.2^{15,18}.2^{25,28}.2^{29,32}]pentaconta-2,7,9,20,-22,33,34,39,41-nonaene-κ^4N)copper(II)] Tetrahexafluorophosphate),

Table VII. Positional Parameters ($\times 10^4$) for [Ni{Me_2(bipiperidiniumyl)$_2$3,6-dur[]16]cyclidene}][PF_6]$_4$·2C_6H_5CN

	x	y	z	10^3U, Å^2		x	y	z	10^3U, Å^2
Ni	1489 (3)	6553 (3)	4997 (1)	59 (2)*	C15	2064 (21)	5369 (17)	6236 (8)	59 (10)
P1	5135 (6)	5548 (5)	2249 (3)	76 (6)*	C16	2586 (19)	4576 (16)	6386 (8)	40 (9)
F11	4264	5158	2354	171 (19)*	C17	1459 (18)	6720 (16)	6397 (7)	47 (9)
F12	6006	5937	2144	193 (20)*	C18	2022 (22)	7315 (18)	6728 (8)	75 (12)
F13	5888	5129	2625	234 (21)*	C19	1960 (21)	7107 (16)	7159 (8)	53 (10)
F14	4382	5967	1874	277 (25)*	C20	2365 (22)	6198 (17)	7246 (9)	84 (12)
F15	5104	6301	2512	179 (19)*	C21	1832 (20)	5632 (17)	6914 (8)	61 (10)
F16	5166	4794	1986	202 (20)*	C22	2525 (20)	7665 (16)	7495 (7)	51 (10)
P2	102 (7)	1707 (5)	1592 (3)	96 (7)*	C23	2303 (21)	8582 (18)	7394 (9)	85 (12)
F21	55	913	1346	166 (17)*	C24	2816 (23)	9124 (21)	7729 (9)	103 (14)
F22	148	2502	1838	140 (14)*	C25	2793 (22)	8099 (16)	8234 (9)	75 (11)
F23	1009	1366	1938	172 (17)*	C26	2318 (23)	7508 (21)	7878 (9)	95 (13)
F24	−805	2049	1245	247 (22)*	C27	2966 (20)	9547 (16)	8456 (8)	47 (9)
F25	−607	1323	1793	228 (24)*	C28	3018 (26)	10420 (21)	8321 (9)	70 (11)
F26	810	2092	1391	210 (22)*	C29	2147 (22)	10888 (19)	8223 (9)	52 (10)
P3	9296 (8)	6427 (7)	810 (4)	116 (8)*	C30	1231 (24)	10651 (21)	5353 (10)	92 (13)
F31	10292	6857	852	232 (24)*	C31	2120 (23)	11601 (21)	7969 (9)	61 (10)
F32	8301	5997	768	249 (6)*	C32	1155 (25)	12129 (20)	7883 (10)	87 (12)
F33	9296	6021	410	245 (26)*	C33	2966 (21)	11798 (19)	7872 (9)	53 (10)
F34	9297	6832	1210	286 (29)*	C34	3919 (19)	11393 (18)	8050 (8)	52 (9)
F35	8717	7166	566	287 (34)*	C35	4829 (22)	11728 (20)	7974 (9)	85 (12)
F36	9876	5688	1054	280 (31)*	C36	3936 (22)	10693 (17)	8291 (8)	44 (9)
P4	4444 (8)	1949 (8)	674 (4)	118 (9)*	C37	4923 (21)	10223 (17)	8449 (8)	52 (10)
F41	4330	1607	248	249 (24)*	C38	2802 (23)	12395 (20)	7537 (9)	83 (12)
F42	4558	2290	1100	280 (27)*	C39	3325 (26)	12067 (23)	6938 (10)	140 (17)
F43	5550	1685	829	394 (39)*	C40	3082 (25)	11814 (20)	6511 (10)	106 (14)
F44	3338	2213	519	305 (30)*	C41	2714 (23)	10920 (20)	6475 (9)	66 (11)
F45	4144	1107	798	336 (38)*	C42	1908 (21)	10836 (19)	6658 (8)	86 (12)
F46	4745	2791	550	346 (37)*	C43	2220 (25)	11165 (21)	7086 (10)	106 (14)
N1	552 (15)	6214 (13)	5212 (6)	51 (8)	C44	2440 (25)	10661 (21)	6043 (10)	101 (13)
N2	2230 (17)	5600 (15)	5229 (8)	59 (8)	C45	3248 (25)	10729 (23)	5853 (10)	133 (16)
N3	2492 (17)	6871 (15)	4794 (7)	76 (9)	C46	2884 (35)	10447 (27)	5389 (13)	245 (27)
N4	831 (19)	7553 (16)	4795 (7)	69 (9)	C47	1898 (23)	9396 (21)	5551 (9)	106 (14)
N5	1819 (17)	5870 (15)	6496 (7)	64 (8)	C48	2176 (21)	9665 (16)	5989 (8)	64 (11)
N6	2548 (16)	8977 (14)	8107 (7)	58 (8)	C49	2919 (28)	9033 (24)	5134 (12)	124 (15)
N7	2586 (18)	12037 (15)	7113 (7)	83 (10)	C50	3914 (25)	9252 (24)	5036 (11)	121 (16)
N8	2609 (24)	9541 (20)	5328 (10)	153 (14)	CS100	8643 (13)	4653 (8)	1772 (5)	137 (17)
C1	−165 (20)	5695 (18)	5743 (8)	54 (10)	CS101	8640	4101	1464	139 (17)
C2	697 (19)	5919 (17)	5577 (8)	47 (9)	CS102	7733	3822	1187	168 (19)
C3	1678 (20)	5598 (17)	5811 (8)	41 (9)	CS103	6829	4095	1218	160 (19)
C4	2322 (21)	5347 (18)	5574 (9)	51 (10)	CS104	6831	4646	1527	161 (19)
C5	2745 (25)	5102 (21)	4992 (10)	71 (11)	CS105	7738	4926	1804	108 (14)
C61	2709 (46)	5435 (37)	4613 (18)	101 (20)	CS106	9566	4937	2054	154 (18)
C62	3681 (84)	5529 (66)	4961 (36)	101 (20)	NS107	10320	5169	2285	188 (17)
C7	2956 (26)	6301 (21)	4569 (11)	93 (13)	CS(2)110	4757 (16)	7519 (10)	928 (4)	110 (14)
C8	2819 (23)	7619 (19)	4847 (9)	81 (12)	CS(2)111	5118	8101	717	190 (22)
C9	2342 (22)	8307 (21)	4944 (10)	86 (12)	CS(2)112	6089	8032	706	190 (22)
C10	1230 (23)	8332 (22)	4840 (9)	92 (12)	CS(2)113	6700	7380	906	229 (25)
C11	617 (25)	9056 (22)	4655 (11)	103 (14)	CS(2)114	6340	6797	1117	258 (29)
C12	−287 (21)	7528 (19)	4577 (10)	92 (12)	CS(2)115	5368	6867	1128	165 (19)
C13	−687 (22)	6675 (19)	4564 (8)	81 (11)	CS(2)116	3768	7589	939	169 (19)
C14	−562 (17)	6288 (17)	4996 (7)	52 (10)	NS(2)117	2960	7647	948	276 (24)

**[Cu{Me_2(bipiperidiniumyl)$_2$3,6-dur[16]cyclidene}](PF_6)$_4$.** Two grams of [Ni{Me_2(bipiperidiniumyl)$_2$3,6-dur[16]cyclidene}](PF_6)$_4$ was slurried in 100 mL of methanol, and dry hydrogen bromide gas was vigorously bubbled through the solution for 15 min upon which the solution went from a clear orange to green to blue. The reaction mixture was reduced in volume to an oil and dissolved in water and an excess of ammonium hexafluorophosphate added. The resulting voluminous whitish precipitate was collected and dried in vacuo. Then 1.8 g (1.3 mmol) of the free ligand was slurried in 75 mL of hot methanol; 0.26 g (1.3 mmol) of copper acetate and 0.36 g (2.6 mmol) of sodium acetate were slurried in 50 mL of hot methanol and added to the solution of free ligand. The resulting brick-red precipitate was collected and recrystallized from acetonitrile/ethanol. The microcrystalline product was ground and dried in vacuo. Yield: 0.8 g (36%). Anal. Calcd for $CuC_{50}H_{80}N_8(PF_6)_4$: C, 41.58; H, 5.63; N, 7.80; Cu, 4.18. Found: C, 41.37; H, 5.25; N, 7.79; Cu, 4.20.

**[(18,25-Dihydro-2,8,10,21,22,33,41,42-octamethyl-3,7,11,18,25,32,35,39-octaazaheptacyclo-[24.7.7.2^{20,23}.2^{11,14}.2^{15,18}.2^{25,28}.2^{29,32}]pentaconta-2,7,9,20,22,33,34,39,41-nonaene-κ^4N)copper(II)] Tetrachloride, [Cu{Me_2(bipiperidiniumyl)$_2$3,6-dur[16]cyclidene}](Cl)$_4$.** A 1.0-g (0.7-mmol) sample of [Cu{Me_2(bipiperidiniumyl)$_2$3,6-dur[16]cyclidene}](PF_6)$_4$ and 0.97 g (3.5 mmol) of tetrabutylammonium chloride were rigorously dried at 10^{-3} Torr and taken into an inert-atmosphere glovebox. The copper complex was dissolved in 20 mL of previously dried acetone, and the tetrabutylammonium chloride, dissolved in 30 mL of dried acetone, was dripped slowly into the copper(II) solution. The resulting voluminous brick-red precipitate was collected and dried in vacuo. Yield: 0.31 g (38%). Anal. Calcd for $CuC_{50}H_{80}N_8(Cl)_3PF_6$·2$CH_3C(O)CH_3$·2$H_2O$: C, 53.46; H, 7.71; N, 8.91; Cu, 5.05. Found: C, 53.51; H, 7.92; N, 8.71; Cu, 4.97.

Physical Measurements. Elemental analyses were performed by Galbraith Laboratories, Inc., Knoxville, TN. The proton NMR spectra of the guest species, in the presence and absence of the paramagnetic Cu(II) host, were acquired at three different frequencies by using Bruker WP200 200-MHz, Bruker WM300 300-MHz, Bruker AM500 500 MHz, and Nicolet NT500 500-MHz NMR spectrometers. Samples were allowed to equilibrate for 30 min at 304 K by using a variable-temperature control unit. Five-millimeter o.d. Wilmad Royal Imperial sample tubes, 528-PP, 7 in. in length, were used to contain the host–guest sample solutions. Aldrich Gold Label 99.96% deuterium oxide, low in paramagnetic impurities, was used as the solvent in all experiments. A 10-μL Hamilton syringe was used to prepare the host–guest solutions. The organic guest molecules used during inclusion complexation experiments were of spectrophotometric grade, Gold Label quality, purchased from Aldrich Chemical Co., and were used without further purification.

Electrochemical data were obtained by using a Princeton Applied Research Corp. Model 173 potentiostat/galvanostat equipped with a Model 175 linear programmer and a Model 179 digital coulometer.

Current vs potential curves were measured on a Houston Instruments Model 200 XY recorder. The working electrode for voltammetric curves was a platinum disk with potentials measured vs. an Ag^0/Ag^+ (0.1 M) reference. Peak potentials were measured from cyclic voltammograms at 100 mv s^{-1} scan rate. Half-wave potentials were taken as the average of the anodic and cathodic peak potentials.

Experimental Precautions. (1) All glassware used in the study of the host–guest phenomena were soaked in 0.5 M EDTA for 24 h prior to use. (2) The deuterium oxide was low in paramagnetic impurities and degassed by freeze–pump–thaw techniques on a vacuum line at 10^{-5} Torr. Guest solutions were also degassed in this manner. (3) All samples for the study of the intramolecular association phenomena were prepared in an inert-atmosphere glovebox and sealed.

Procedure for Host–Guest Studies. (1) A stock solution of the host compound was prepared by accurately weighing an amount of the chloride salt of the host species and dissolving the complex in a 5-mL volumetric flask containing deuterium oxide (typically 1.5×10^{-2} M). (2) A 10-μL syringe was used to deliver an aliquot of the stock host solution into a 2-mL volumetric flask, containing, typically, 150–700 times the concentration of guest. Samples were then drawn and placed into the two 5-nm NMR sample tubes. (3) Measurements of T_{1p} were achieved by two sets of standard inversion recovery experiments obtained at each of three different frequencies. At least 12 different values of the variable delay parameter were used to determine accurately the relaxation times. The program used to calculate T_1 values was from the Bruker library of software programs, (Invrec.Au), and the errors indicated in the table are standard deviations of the fit. The equation to which the points are fit is $Y = A_3 - A_2 \exp(-T/T_1)$, where A_3 = the normalized intensity of the largest point, A_2 = the nucleus flip angle in units of $\pi/2$, and $T = \tau$ value. The convergence limit was set to 1.0×10^{-5}, which provided a very accurate fit to the data. These measurements are discussed in greater detail in ref 9.

Crystal Structure of [Ni[Me_2(bipiperidiniumyl)$_2$3,6-dur[16]-cyclidene]]$(PF_6)_4$ (IIIa). Crystal data for $[NiC_{50}H_{104}N_8](PF_6)_4 \cdot 2C_6H_5CN$: M_r = 1638.0, monoclinic, space group $P2_1/c$, a = 14.172 (4) Å, b = 16.235 (5) Å, c = 34.705 (10) Å, β = 109.76 (2)°, V = 7515 (4) Å^3, Z = 4, ρ = 1.45 g cm^{-3}, Mo Kα radiation, λ = 0.71069 Å, T = 299 K, μ(Mo Kα) = 4.45 cm^{-1}, $F(000)$ = 3480, $R(F_o)$ = 0.112, $R_w(F_o)$ = 0.12.

Crystal character: orange-red plates obtained by recrystallization from benzonitrile. Data were collected with a Syntex $P2_1$ four-circle diffractometer. Maximum 2θ = 40°, with a scan range from −0.9 + 1.0(2θ) around the $K\alpha_1$ – $K\alpha_2$ angles; scan speed = 2–29° min^{-1}, depending on the intensity of a 2-s prescan; backgrounds were measured at each end of the scan for 0.25 of the scan time. *hkl* ranges: 0 to 13; 0 to 15; −33 to +33.

Three standard reflections were monitored every 200 reflections and showed no changes during data collection. Unit cell dimensions and standard deviations were obtained by least-squares fit to 15 reflections ($16 < 2\theta < 20°$). Merging gave 7052 unique reflections (R_{init} = 0.05). A total of 1775 were considered observed ($I/\sigma(I) \geq 2.5$) and used in refinement; they were corrected for Lorentz and polarization but not absorption effects. Crystal dimensions were 0.07 × 0.2 × 0.4 mm. Systematic absences $h0l$, $l = 2n$, $0k0$, $k = 2n$, indicate space group $P2_1/c$.

Solution and Refinement of the Crystal Structure. The Ni atom position was readily located from a Patterson synthesis, but initial Fourier syntheses showed no chemically recognizable structures. Additional atoms were found by the SHELXTL FIND procedure, involving recycling the peaks on sequential E maps. After 10 cycles, 55 atomic positions had been found, which were virtually all correct. Remaining light atoms were then found on successive Fourier syntheses, including two molecules of benzonitrile (given ideal geometry in final refinement). PF_6 groups were held as rigid octahedra (P–F = 1.536 Å). Anisotropic temperature factors were used otherwise only for Ni, P, and F. Hydrogen atoms were given fixed isotropic temperature factors, U = 0.07 Å^2. Those defined by the molecular geometry were inserted at calculated positions and not refined; H atoms of methyl groups were omitted. One atom (C6) was disordered, with refined occupancies 0.65 (3) and 0.35 (3); H atoms attached to C5 to C7 were included only for the higher occupancy component. A total of 445 parameters were refined.

Final refinement was on F by cascaded least-squares methods. A weighting scheme of the form $w = 1/\sigma^2(F) + gF^2$ with g = 0.0011 was used and shown to be satisfactory by a weight analysis. Final $R(F_o)$ = 0.112, $R_w(F_o)$ = 0.12. Maximum shift/error in final cycle was 0.2. Largest positive and negative peaks on a final difference Fourier synthesis were of height 0.5 e Å^{-3}. The relatively high final R value is clearly due to the poor diffracting power (responsible also for the low ratio of observed to total reflections despite the low $2\theta_{max}$) and to the poorly ordered PF_6^- groups.

Computations used SHELXTL[24] on a Data General DB30 computer, apart from data reduction on a Burroughs B6800 computer. Scattering factors in the analytical form and anomalous dispersion factors were taken from ref 25. Final atomic coordinates are given in Table VII, and bond lengths and angles are given in Tables II and III.

Acknowledgment. The financial support of the National Institutes of Health, Grant No. GM10040, and the National Science Foundation, Grant No. CHE-8822822, is greatly appreciated. We also thank Dr. K. Goldsby for acquiring and interpreting the electrochemical data and Dr. N. Herron for providing the ChemGraph illustration. FT-NMR spectra at 11.75 T (500 MHz) and 7.0 T (300 MHz) were obtained at The Ohio State University Chemical Instrument Center on equipment funded in part by NIH Grant No. 1 510 RR01458-01A1.

Supplementary Material Available: Anisotropic thermal parameters (Table S2) and H atom coordinates (Table S3) (3 pages); listings of structure factors (Table S1) (11 pages). Ordering information is given on any current masthead page.

(24) Sheldrick, G. M. *SHELXTL Users Manual*; Nicolet Instrument Co.: Madison, WI, 1983.
(25) *International Tables for X-Ray Crystallography*, Kynoch: Birmingham, England, 1974; Vol. IV.